Tolvaptan plus Pasireotide Shows Enhanced Efficacy in a PKD1 Model

Katharina Hopp,* Cynthia J. Hommerding,* Xiaofang Wang,* Hong Ye,* Peter C. Harris,*† and Vicente E. Torres*

*Division of Nephrology and Hypertension and †Department of Biochemistry and Molecular Biology, Mayo Clinic, Rochester, Minnesota

ABSTRACT

Autosomal dominant polycystic kidney disease (ADPKD) is a leading cause of ESRD. A central defect associated with ADPKD pathology is elevated levels of 3′, 5′-cyclic AMP (cAMP). Compounds such as tolvaptan and pasireotide, which indirectly reduce adenylyl cyclase 6 (AC6) activity, have hence proven effective in slowing cyst progression. Here, we tested the efficacy of these compounds individually and in combination in a hypomorphic PKD1 model, *Pkd1*$^{R3277C/R3277C}$ (*Pkd1*$^{RC/RC}$), in a 5-month preclinical trial. Initially, the *Pkd1*$^{RC/RC}$ model was inbred into the C57BL/6 background, minimizing disease variability, and the pathogenic effect of elevating cAMP was confirmed by treatment with the AC6 stimulant desmopressin. Treatment with tolvaptan or pasireotide alone markedly reduced cyst progression and in combination showed a clear additive effect. Furthermore, combination treatment significantly reduced cystic and fibrotic volume and decreased cAMP to wild-type levels. We also showed that *Pkd1*$^{RC/RC}$ mice experience hepatic hypertrophy that can be corrected by pasireotide. The observed additive effect reinforces the central role of AC6 and cAMP in ADPKD pathogenesis and highlights the likely benefit of combination therapy for patients with ADPKD.

J Am Soc Nephrol 26: 39–47, 2015. doi: 10.1681/ASN.2013121312

Autosomal dominant polycystic kidney disease (ADPKD) is the most common monogenic nephropathy and the fourth leading cause of ESRD. It is characterized by progressive development of bilateral renal cysts, often accompanied by liver cysts and an increased risk for vascular abnormalities. ADPKD is caused by mutations to *PKD1* or *PKD2*, encoding polycystin-1 or -2 (PC1/2).[1,2] The polycystins are thought to form a complex that regulates Ca^{2+} influx in response to extracellular mechanical or chemical stimuli.[3] Decreased intracellular Ca^{2+} levels result in downregulation of calcium-dependent phosphodiesterases and stimulation of calcium-inhibitable adenylyl cyclase 6 (AC6).[4–6] As a consequence, elevated 3′,5′-cyclic AMP (cAMP) levels have been found in various murine PKD models.[7–11] cAMP stimulates protein kinase A–mediated signaling and leads to increased fluid secretion, proliferation/dedifferentiation, and disrupted flow sensing/tubulogenesis—key features of cystogenesis.[12–14] Hence, lowering intracellular cAMP levels has been a major focus in the development of therapeutic interventions for ADPKD.[14]

Multiple murine and human trials have indirectly targeted AC6, the AC isoform predominant in collecting duct principal cells, through the arginine vasopressin receptor 2 (AVPR2) or the somatostatin receptors (SSTR1–SSTR5).[15,16] Binding of circulating vasopressin to AVPR2 stimulates AC6 by coupling through guanosine nucleotide–binding (G)-stimulatory proteins,[17] and AVPR2 antagonists have alleviated cyst burden in preclinical[8,18–21] and clinical[22,23] trials. The most prominently used AVPR2 antagonist is tolvaptan, which has shown efficacy in multiple rodent models, and a long-term clinical trial of 1445 patients that reported a 2.8%/year increase in total kidney volume in the treated population compared with 5.5%/year in the placebo group.[23] SSTRs inhibit AC6 activity through G-inhibitory proteins and are activated by the peptide hormone somatostatin.[24,25] Because of the short half-life of somatostatin, more stable synthetic analogues have been tested in preclinical and clinical trials. Octreotide or lanreotide, which bind to SSTR2 and -3, have been tested in murine studies[26,27] and small clinical trials, in which they slowed renal and hepatic cyst expansion.[28–31] The recently developed pasireotide binds to SSTR1, -2, -3, and -5 and has shown enhanced efficacy over octreotide in the *Pkd2*$^{-/WS25}$ mouse and PCK rat models.[27] Despite the promising results, no treatment for ADPKD has been

Received December 17, 2013. Accepted May 14, 2014.

Published online ahead of print. Publication date available at www.jasn.org.

Correspondence: Dr. Vicente E. Torres, Division of Nephrology and Hypertension, Mayo Clinic, 200 First Street SW, Rochester, MN 55905. Email: torres.vicente@mayo.edu

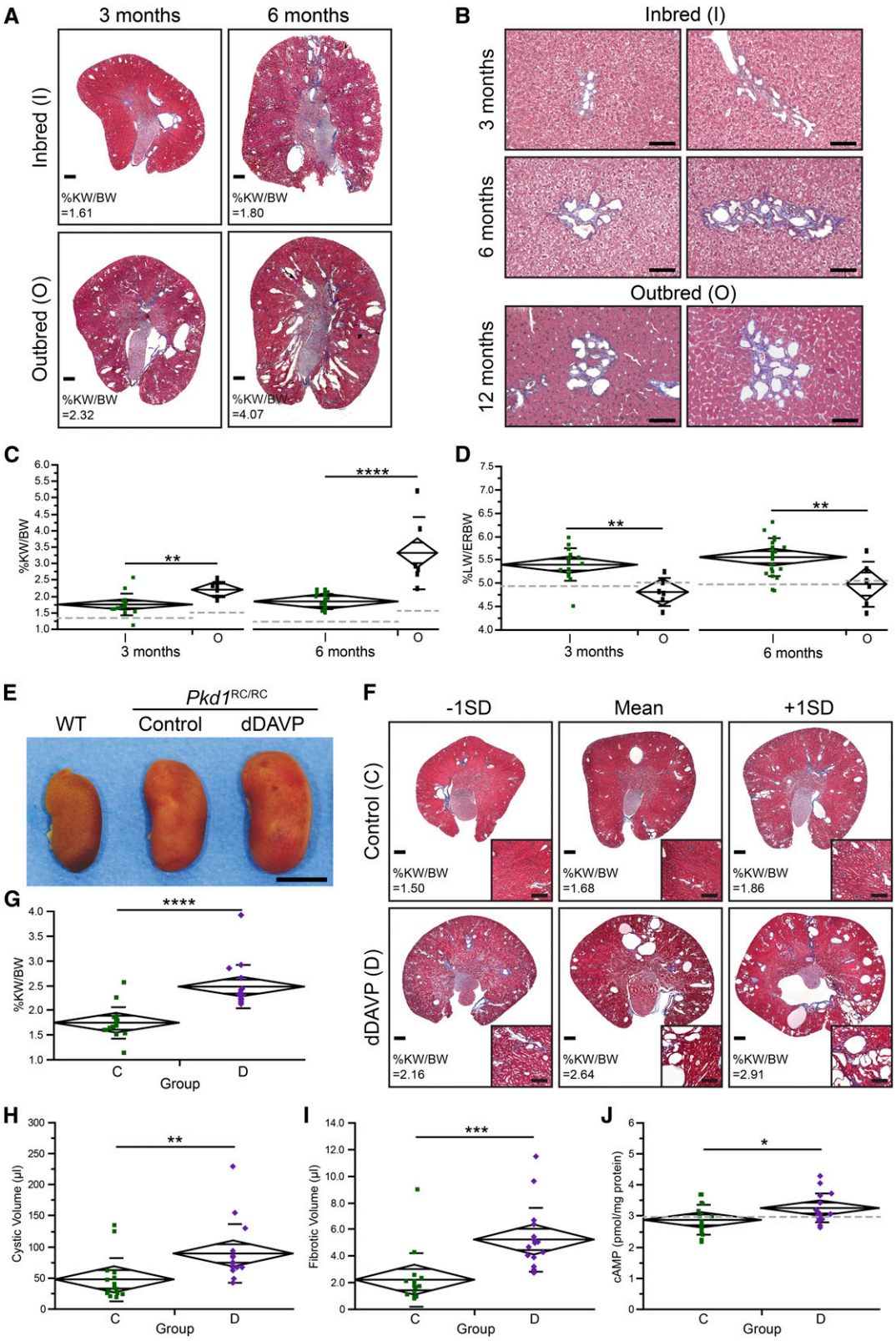

Figure 1. C57BL/6 *Pkd1*$^{RC/RC}$ mice have milder PKD than the outbred model and respond to dDAVP treatment. (A) Masson's trichrome–stained kidney cross-sections of 3-month-old or 6-month-old inbred and outbred animals. Outbred animals developed higher cyst burdens and larger kidneys compared with inbred mice. Scale bar: 500 μm. (B) Masson's trichrome–stained liver sections of microhamartomas (small, dilated, irregularly shaped bile ducts surrounded by fibrosis). In outbred animals this abnormality was not found before

approved to date. Here we performed a preclinical study to test whether tolvaptan and pasireotide combination therapy has enhanced efficacy over single drug treatments.

The preclinical study was performed in the homozygous *Pkd1*$^{R3277C/R3277C}$ (*Pkd1*$^{RC/RC}$) model, which closely mimics human ADPKD with slowly progressive PKD, but to minimize phenotypic variability the outbred 129S6; C57BL/6 *Pkd1* RC model[11] was fully inbred into the C57BL/6 background. The progression of PKD of inbred *Pkd1*$^{RC/RC}$ mice, while more consistent, was milder and slower than in the previously published outbred model (Figure 1, A and C). However, cysts continued to originate primarily from collecting ducts (percentage of cysts: proximal tubule, 12%; collecting duct, 69%; unstained, 19%; ANOVA: $P=9.85\times10^{-6}$) (Supplemental Figure 1, F and G). At three months, the percentage of kidney weight/body weight (%KW/body wt) was 1.74% ±0.32% in the inbred animals ($n=16$) and 2.19%±0.24% in the outbred mice ($n=6$; $P=0.54\times10^{-2}$). This difference became even more significant at 6 months (%KW/body wt: inbred [$n=22$], 1.87%±0.23%; outbread [$n=6$], 3.35%±1.10%; $P=3.73\times10^{-6}$), although there was much less variability (Figure 1C). Despite slower progression, %KW/body wt of inbred mice steadily increased with age and BUN levels were significantly elevated at 9 months, as previously reported in the outbred background (Supplemental Figure 1, B–E).[11] A significant sex difference was noted starting at 9 months, with females having more severe disease, an effect likely correlated to the C57BL/6 genetic background. In addition, inbred mice had a higher percentage of liver weight/extrarenal body weight (%LW/ERbody wt) and developed microhamartomas as early as 3 months, compared with 12 months in the outbred background (Figure 1, B and D), highlighting that genetic background effects can vary depending on the organ.

To test the pathogenic role of cAMP in the inbred *Pkd1*$^{RC/RC}$ model, mice were treated from 1 to 3 months with the synthetic vasopressin analogue desmopressin (dDAVP) to increase cAMP levels.[20] Gross anatomy and Masson's trichrome–stained kidney sections showed a higher cyst burden in dDAVP-treated mice ($n=16$) than in untreated controls ($n=16$) (Figure 1, E and F). This was further reflected in %KW/body wt, which was significantly elevated in the treated group (%KW/body wt: control, 1.74% ±0.32%; dDAVP, 2.47%±0.45%; $P=1.62\times10^{-5}$) (Figure 1G). Corresponding cystic and fibrotic volumes were also significantly increased in the dDAVP-treated mice (cystic volume: 47.00± 34.86 μl in controls versus 88.64± 46.49 μl in dDAVP mice [$P=0.92\times10^{-2}$]; fibrotic volume: 2.19±2.00 μl versus 5.21±2.40 μl [$P=0.81\times10^{-3}$]) (Figure 1, H and I) and cAMP levels were significantly higher (2.86±0.49 pmol/mg protein versus 3.24±0.47 pmol/mg protein; $P=0.29\times10^{-1}$) (Figure 1J). The %LW/ERbody wt did not differ between the groups, and no sex difference was observed. Together, these results reemphasized the central role of cAMP in cyst progression/development in PKD1 and confirmed the suitability of the inbred *Pkd1*$^{RC/RC}$ model for preclinical trials.

To evaluate the benefit of tolvaptan, pasireotide, or combination treatment in slowing PKD progression, inbred *Pkd1*$^{RC/RC}$ mice were treated from 1 to 6 months. This long-term treatment was chosen to better mimic comparable treatment of patients with ADPKD, to adequately evaluate the efficacy of the combination therapy, and to assess potential adverse events. At the time of euthanasia, gross anatomic comparisons between kidneys of untreated control ($n=22$), tolvaptan-treated mice ($n=21$), pasireotide-treated mice ($n=18$), and tolvaptan plus pasireotide–treated mice ($n=20$) showed a clear reduction in kidney size of mice treated with either drug alone, with an even greater reduction (back to the size of wild-type [WT] kidneys) in combination-treated animals (Figure 2A). This observation correlated with the histologic analysis and %KW/body wt (Figure 2, B–D, Table 1, Supplemental Figure 2). Pairwise comparisons showed the greatest significance for the combined

12 months, but inbred mice developed similar-size microhamartomas as early as 3 months. Scale bar: 100 μm. (C and D) %KW/body wt and %LW/ERbody wt of inbred (green) and outbred (black) mice at 3 and 6 months, depicted as mean diamonds and SDs. (C) The %KW/body wt in inbred mice was less variable among non-littermates but overall was milder and more slowly progressive. Wild-type (WT) C57BL/6 mice also had lower %KW/body wt than WT outbred mice, while body weight remained constant, highlighting a clear background effect in kidney anatomy (%KW/body wt in 10 inbred mice and 4 outbred mice: 3 months, inbred, 1.35%±0.11%, outbred, 1.49%±0.20% [$P=0.11$]; 6 months, inbred, 1.24%±0.05%, outbred, 1.66±0.24 [$P=0.15\times10^{-3}$) (Supplemental Figure 1A). (D) The %LW/ERbody wt was elevated in inbred compared with outbred mice at 3 months (inbred, 5.39%±0.34%; outbred, 4.80%±0.30%; $P=0.21\times10^{-2}$) and 6 months (inbred, 5.54%±0.40%; outbred, 4.97%±0.48%; $P=0.34\times10^{-2}$). Gray dotted lines represent WT (C57BL/6 or outbred) mice. (E) Gross anatomy of representative kidneys from inbred WT mice, inbred *Pkd1*$^{RC/RC}$ control mice, and dDAVP-treated mice (6 months of age) highlights increased kidney size after dDAVP treatment. Scale bar: 0.5 cm. (F) Masson's trichrome–stained cross-sections of kidneys with mean±1×SD %KW/body wt. Cross-sections of dDAVP-treated mice showed more severe cystic disease with dilated tubules/ducts (inset, cortex) compared with untreated mice. Scale bar: 500 μm, 250 μm (inset). (G–J) %KW/body wt (G), renal cystic volume (H), renal fibrotic volume (I), and cAMP levels (J) of saline-treated inbred *Pkd1*$^{RC/RC}$ control mice (C, green) and dDAVP-treated mice (D, purple), depicted as mean diamonds and SDs. Gray dotted lines represent WT values. dDAVP treatment significantly increased %KW/body wt (G), cystic volume (H), and fibrotic volume (I). (J) As predicted, cAMP levels were elevated upon dDAVP treatment. %KW/BW, %KW/body wt. *$P<0.05$; ** $P<0.01$; ***$P<0.001$; ****$P<0.0001$. Data of outbred animals were obtained from reference 11.

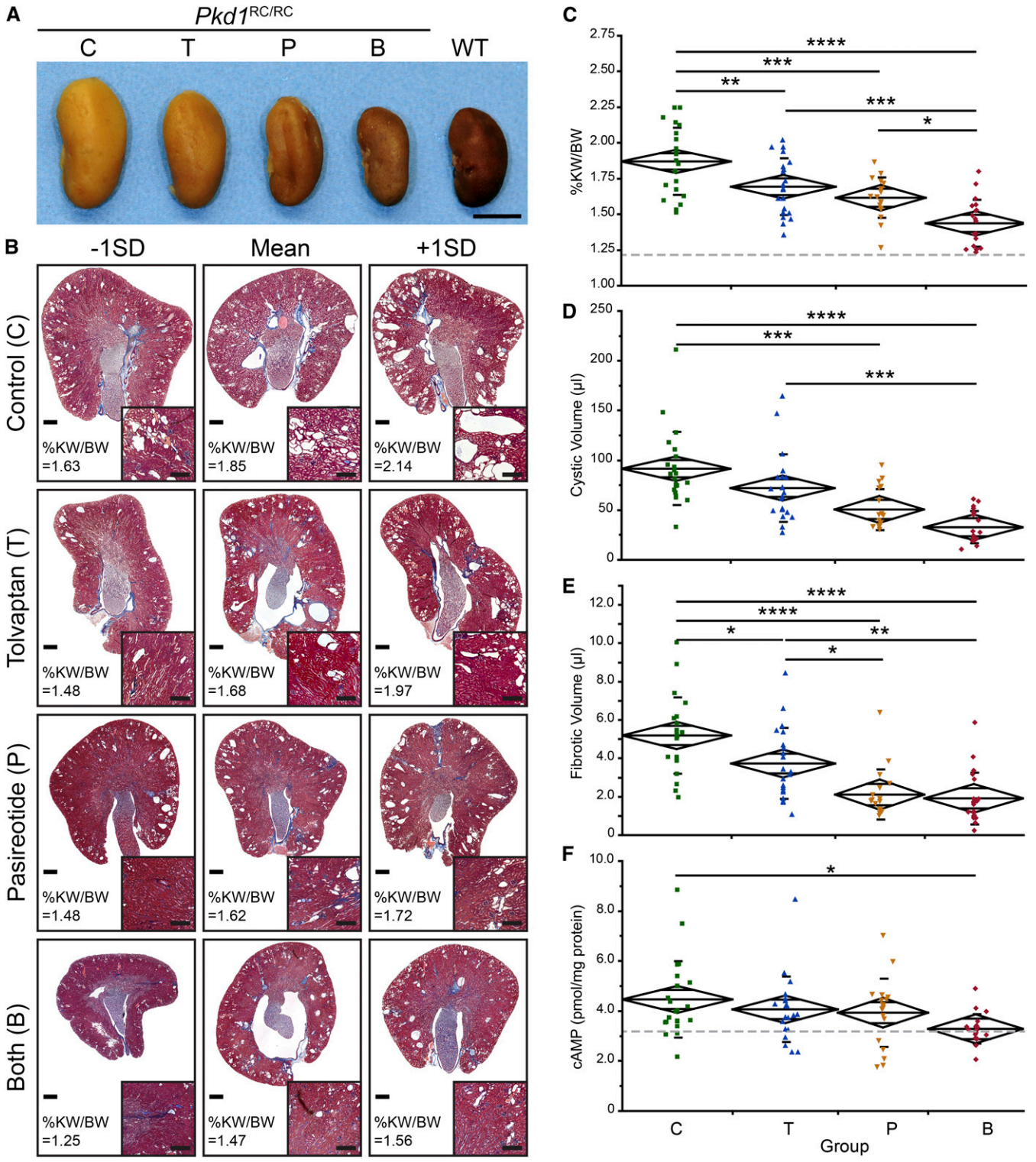

Figure 2. Tolvaptan plus pasireotide treatment showed enhanced efficacy over single drug treatment. (A) Gross anatomy of representative kidneys from inbred WT and inbred *Pkd1*$^{RC/RC}$ control mice, C; tolvaptan-treated mice, T; pasireotide-treated mice, P; and tolvaptan plus pasireotide–treated mice, B (6 months of age). Treatment with both drugs showed a clear additive effect, reducing kidney size back to WT range. Scale bar: 0.5 cm. (B) Masson's trichrome–stained cross-sections of kidneys with mean±1×SD %KW/body wt. Untreated animals showed multiple cysts and dilated tubules/ducts (inset, cortex) (Supplemental Figure 2). Cyst burden and dilations were reduced upon treatment with either drug alone and were nearly eliminated by combination therapy (Supplemental Figure 2). Scale bar: 500 μm, 250μm (inset). (C–F) %KW/body wt (C), renal cystic volume (D), renal fibrotic volume (E), and cAMP levels (F) of saline-treated *Pkd1*$^{RC/RC}$

treatment with a marked additive effect over single treatments (Table 1). Masson's trichrome–stained kidney sections showed a reduction in size/number of cysts and dilated tubules/ducts in tolvaptan- or pasireotide-treated mice and only a few cysts with mainly normal-appearing cortex and medulla in animals treated with both drugs (Figure 2B, inset, Supplemental Figure 2). This was further reflected in the overall cystic volume, which was significantly reduced upon single or combination treatment (Figure 2D, Table 1). In addition, treatment with tolvaptan significantly reduced fibrotic volume, which was even further decreased by treatment with pasireotide or both drugs (Figure 2E, Table 1). Consistent with the target of the treatments, cAMP levels were significantly reduced back to WT levels by the combination treatment (WT, 3.25±0.88 pmol/mg protein) (Figure 2F, Table 1). None of the treatments resulted in clear adverse events (see Concise Methods), even though body weight decreased slightly upon treatment with pasireotide alone or combined with tolvaptan (WT, 26.46±3.75 g) (Table 1). No significant difference was noted in BUN, which was in the WT range at 6 months of age (Supplemental Figure 1E), and no significant sex effects were observed.

In addition to the alleviating effect of pasireotide on renal abnormalities, the drug also reduced urinary output, counteracting the tolvaptan-induced polyuria in animals treated with both drugs (Supplemental Table 1).[23] While the mechanism for this antidiuretic effect of pasireotide is unclear, similar effects have been reported in patients treated with somatostatin.[32,33] This may highlight a favorable effect of the combination treatment because polyuria is considered an adverse event of tolvaptan treatment and the reason for treatment discontinuation in 8.3% of patients in a recently published trial[23]; however, more detailed studies are required.

Treatment with pasireotide reduced %LW/ERbody wt back to WT levels (WT, 4.92%±0.32%) (Figure 3A, Table 1). Because the observed microhamartomas of untreated animals were small, few in number, and also found in pasireotide-treated mice (data not shown), it was unlikely that the reduction of %LW/ERbody wt correlated to this particular abnormality. The effect of a reduction of PC1 on hepatocyte morphology is unknown. However, it has been reported that SSTR2 and SSTR4 are expressed in hepatocyte cell lines and that all SSTRs mislocalize to hepatocytes in pathologic conditions.[34,35] Consequently, we evaluated whether hepatocyte hypertrophy or hyperplasia may underlie the increase in %LW/ERbody wt. Measuring DNA content per milligram of liver tissue, which was reduced in control animals versus pasireotide-treated and WT mice (data not shown), and counting nuclei per 0.01 mm^2, highlighted that C57BL/6 *Pkd1*$^{RC/RC}$ animals experienced hepatocyte hypertrophy, which was corrected by pasireotide treatment (Figure 3, B and C). To date, hepatic hypertrophy has not been reported as a pathologic feature of ADPKD; elevated liver weights have been seen in patients but have been correlated only to cyst burden and not hepatocyte size. Because AVPR2 is not expressed in the liver, it was not surprising that tolvaptan did not decrease %LW/ERbody wt.

We have demonstrated in a slowly progressive model of PKD1 the value of treatment with tolvaptan or pasireotide alone and the additive effect of combined therapy, suggesting that using two means to lower cAMP levels would be beneficial in the human disease. Using the combination of both drugs may also allow lower single drug doses, achieving similar results but limiting adverse events. The benefit was seen in terms of %KW/body wt, cystic and fibrotic volumes, and cAMP levels for the combined treatment. Renal function did not significantly differ because these inbred animals had relatively mild disease. However, correlations between the significant endpoints found here and reduction in BUN in older outbred and inbred animals (Supplemental Figure 1E) of this model suggest that renal function differences would have been seen if the study had been extended.[11] This is analogous to the correlation between total kidney volume in young patients and a subsequent decline in renal function that has been established in human ADPKD.[36] Interestingly, the effect of pasireotide was generally greater than for tolvaptan, and this may be because of the slow, even release from the minipump compared with the nightly ingestion of tolvaptan in food; this effect suggests that a split dose or slow-release AVPR2 antagonist may provide further benefit. In addition, pasireotide treatment showed a slight antidiuretic effect, which may benefit patients treated with both drugs because it could reduce aquaresis-related symptoms induced by tolvaptan. Further, pasireotide corrects the hepatic hypertrophy observed in the inbred *PKD1*$^{RC/RC}$ model, an abnormality that may be present but unrecognized in patients, masked by polycystic liver disease.

CONCISE METHODS

Inbreeding of the *Pkd1*$^{RC/RC}$ Model into the C57BL/6 Background

The animals were inbred into the C57BL/6 background using the IDEXX RADIL speed congenic service. First, the sex chromosomes were fixed, followed by microsatellite analysis of the autosomes. Animals were considered inbred when all of the microsatellite markers

controls (green), tolvaptan-treated (blue), pasireotide-treated (yellow), and tolvaptan plus pasireotide–treated mice (red) depicted as mean diamonds and SD. Gray dotted lines represent WT C57BL/6 values. (C) The %KW/body wt was significantly decreased by treatment with either drug alone and even further decreased with use of the combination. (D and E) Similar trends were observed for cystic and fibrotic volume. For these two parameters, pasireotide slightly outperformed tolvaptan. (F) cAMP levels were only significantly different (back to WT levels) in the combination treatment group, highlighting the importance of the additive effect. %KW/BW, %KW/body wt. *$P<0.05$; **$P<0.01$; ***$P<0.001$; ****$P<0.0001$.

Table 1. Summary of measurements for the combination treatment preclinical trial

Group[a]	Measurements±SD	*P* Values[b]			
		C (*n*=22)	T (*n*=21)	P (*n*=18)	B (*n*=20)
%KW/body wt					
C	1.87±0.23	–	0.01017[b]	0.00023[b]	5.51E-10[b]
T	1.69±0.20	0.01017[b]	–	0.58514	0.00019[b]
P	1.61±0.14	0.00023[b]	0.58514	–	0.01832[b]
B	1.43±0.16	5.51E-10[b]	0.00019[b]	0.01832[b]	–
%LW/ERbody wt					
C	5.54±0.40	–	0.86211	1.23E-06[b]	4.91E-07[b]
T	5.60±0.34	0.86211	–	7.48E-08[b]	2.75E-08[b]
P	4.96±0.43	1.23E-06[b]	7.48E-08[b]	–	0.99986
B	4.94±0.29	4.91E-07[b]	2.75E-08[b]	0.99986	–
Cystic volume (μl)					
C	91.31±36.73	–	0.14538	0.00018[b]	5.16E-08[b]
T	71.85±34.19	0.14538	–	0.09899	0.00027[b]
P	50.37±20.58	0.00018[b]	0.09899	–	0.25587
B	32.48±16.17	5.16E-08[b]	0.00027[b]	0.25587	–
Fibrotic volume (μl)					
C	5.18±1.98	–	0.02634[b]	4.33E-07[b]	7.26E-08[b]
T	3.72±1.85	0.02634[b]	–	0.01107[b]	0.00381[b]
P	2.10±1.31	4.33E-07[b]	0.01107[b]	–	0.99367
B	1.90±1.35	7.26E-08[b]	0.00381[b]	0.99367	–
cAMP (pmol/μg protein)					
C	4.45±1.53	–	0.68829	0.54057	0.01671[b]
T	4.06±1.32	0.68829	–	0.99251	0.21733
P	3.92±1.37	0.54057	0.99251	–	0.38158
B	3.28±0.59	0.01671[b]	0.21733	0.38158	–
Body wt (g)					
C	26.32±3.17	–	0.92433	6.71E-06[b]	4.32E-10[b]
T	25.72±3.90	0.92433	–	0.00018[b]	4.79E-10[b]
P	23.39±2.27	6.71E-06[b]	0.00018[b]	–	0.01202[b]
B	21.37±2.23	4.32E-10[b]	4.79E-10[b]	0.01202[b]	–

C, control (*Pkd1*$^{RC/RC}$, untreated); T, tolvaptan; P, pasireotide; B, both (tolvaptan plus pasireotide).
[a]Six-month-old inbred animals.
[b]Significant at $P<0.05$.

matched the C57BL/6 strain. Thereafter, animals were maintained as homozygotes.

Experimental Animals and Study Design

The Institutional Animal Care and Utilization Committee approved the use of the C57BL/6 *Pkd1*$^{RC/RC}$ model, maintained at the animal facilities of the Mayo Clinic, Rochester, MN, and all experimental protocols described in this report.

Desmopressin Treatment

Inbred *Pkd1*$^{RC/RC}$ mice were divided into a control group and a treatment group at 3 weeks of age (n=32; eight animals per treatment group and sex). Littermates of the same sex were sorted into different treatment groups. From 1 to 3 months of age, animals received saline or dDAVP (30 ng/100 g body weight per hour) (V1005, Sigma-Aldrich) *via* osmotic minipump (Alzet model 1004) as described previously.[37] The minipumps were replaced every 3 weeks, and all animals survived the trial period.

Tolvaptan and Pasireotide Treatment

Inbred *Pkd1*$^{RC/RC}$ mice were divided into four groups (control, tolvaptan, pasireotide, tolvaptan plus pasireotide) at 3 weeks of age (n=88; 11 animals per treatment per sex). Littermates of the same sex were sorted into different treatment groups. Treatment with tolvaptan and/or pasireotide was started at 1 month of age, and all animals were euthanized at 6 months of age. Tolvaptan-treated animals received 0.1% tolvaptan (Otsuka Pharmaceuticals) in their ground rodent chow, by homogenous mixing, whereas control animals and those treated only with pasireotide received the same diet without the drug. Pasireotide (Novartis) was administered by osmotic minipump at a dosage of 10 μg/1 kg body weight per hour. The minipump of control animals and those receiving only tolvaptan contained saline. All minipumps were replaced every 3 weeks.

Urine Collection/Analysis

One week before euthanasia, all animals in each treatment group and the control group were placed in a metabolic cage from 6 pm to 6 am (in each group, two to four mice were combined in one metabolic cage). Urine volumes were recorded the next morning and osmolality was measured using pHOx Ultra (Nova Biomedical).

Tissue and Blood Harvest/Analysis

The animals were euthanized by CO_2 exposure, and the body weight of each animal was recorded. Blood was then collected *via* cardiac puncture, and kidneys, liver, spleen, and heart were harvested and weighed. The left kidney and small pieces of each liver lobe were flash frozen, and the right kidney plus all other organs were fixed in 4% paraformaldehyde. For the tolvaptan/pasireotide trial, total blood was used for a complete chemistry and electrolyte analysis measuring 14 variables (Abaxis, VetScanVS2, Comprehensive Diagnostic Panel). This panel included BUN and a liver function test quantifying aspartate aminotransferase, alanine aminotransferase, and alkaline phosphatase. All BUN values were in the range of WT values. The aspartate aminotransferase and alanine aminotransferase values did not significantly differ from WT values, and alkaline phosphatase values in the control and tolvaptan-treated mice were slightly lower than WT values but within normal range (normal ranges provided by VetScanVS2 profiles). BUN levels of animals beyond 6 months of age were measured using pHOx Ultra.

Histomorphometric Analysis

Cystic volumes and fibrotic volumes were calculated as previously described[20] using three cross-sections per kidney. In short, the cystic volume was calculated by measuring the percentage cystic area of the three cross-sections, adjusted to kidney weight

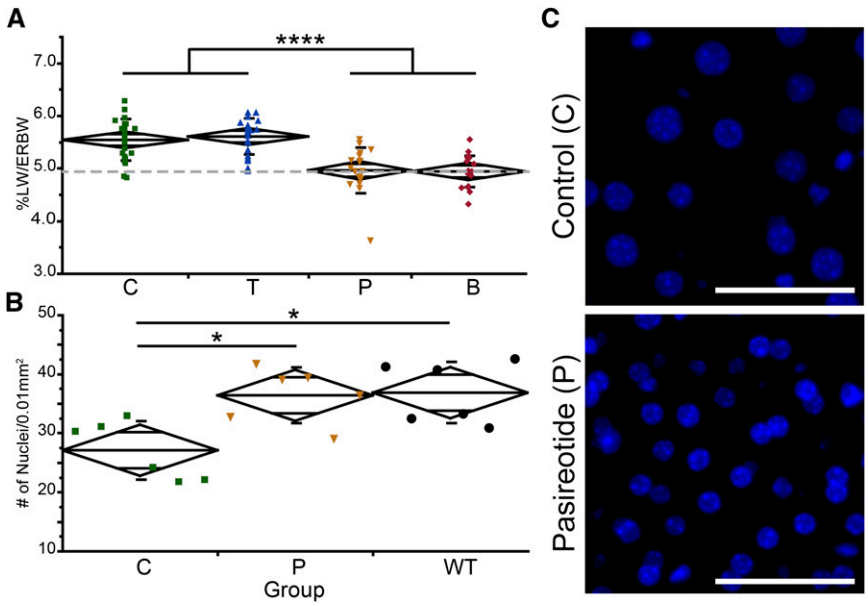

Figure 3. Hepatic hypertrophy of *Pkd1*$^{RC/RC}$ mice can be corrected by pasireotide treatment. (A) %LW/ERbody wt of saline treated, inbred *Pkd1*$^{RC/RC}$ control mice (C, green), tolvaptan-treated mice (T, blue), pasireotide-treated mice (P, yellow), and tolvaptan plus pasireotide–treated mice (B, red) (6 months of age) depicted as mean diamonds and SD. Gray dotted line represents C57BL/6 WT value. The %LW/ERbody wt returned to WT level in animals treated with pasireotide. (B) Number of DAPI-positive nuclei per 0.01 mm^2 in liver cross-sections of *Pkd1*$^{RC/RC}$ controls (green), pasireotide-treated mice (yellow), and WT mice (black), depicted as mean diamonds and SD. Per given area, untreated animals had fewer nuclei compared with pasireotide-treated or WT animals, indicative of larger cells (hypertrophy). (C) Representative image of part B. Scale bar: 50 μm. Hepatic hypertrophy has not previously been reported as a characteristic of ADPKD. Because both PC1 and PC2 are expressed in hepatocytes (Supplemental Figure 3), reduced expression or function of PC1 may be the cause for the observed higher %LW/ERbody wt. %LW/ERBW, %LW/ERbody wt. *P<0.05; ****P<0.0001.

(approximate kidney volume). Fibrotic volume was calculated from the percentage fibrotic area of 10 cortical images and adjusted to kidney weight (approximate kidney volume). Hepatic hypertrophy was evaluated using three females and three males with average %LW/ERbody wt. DNA was isolated from frozen tissue originating from two different lobes using the DNeasy Blood & Tissue kit from Qiagen. Before isolation, the tissue was weighed and the isolated DNA was quantified in duplicates using the Qubit 2.0 fluorometer. For the nuclear counts, tissue was stained with DAPI as previously described.[11] Fifteen ×40 images from three different liver lobes (five images per lobe) were taken using the Zeiss AxioObserver and quantified using the Zen software (Carl Zeiss). All histologic images were taken as previously described.[11]

Evaluation of Adverse Events of Tolvaptan/Pasireotide-Treated Animals

Because the trial required numerous pump replacements, five animals died immediately after surgery or within the following 2 days (one in the tolvaptan group, three in the pasireotide group, and one in the combination treatment group). These deaths were probably not drug-related, so death was not considered an adverse event. At the time of euthanasia, every animal was inspected for gross health issues. Body weight had decreased slightly in animals treated with pasireotide and the drug combination (Table 1). However, no notable differences in feeding/drinking habits were observed; thus, the underlying cause and significance of this observation remains unknown. In addition, two animals presented with one severely dysplastic kidney (one in the pasireotide group and one in the combination treatment group) and hence were excluded from the analysis. No other gross anomalous abnormalities were observed, and no abnormalities were noted from the histologic analysis. The blood panel (Abaxis, VetScanVS2, Comprehensive Diagnostic Panel) was used to evaluate potential ion imbalances as well as liver toxicity. No significant differences were noted upon treatment with either drug alone or the combination. Consequently, no definite adverse events were noted within our study.

Immunofluorescence Labeling/ Analysis

Tissue were prepared for immunofluorescence labeling as previously described.[11] Biotinylated-LTA (1:500; Vector Laboratories) and Aqp2 (1:100; Santa Cruz Biotechnology) were used as proximal tubule and collecting duct markers, respectively. Staining against Tamm-Horsfall protein (1:200; Santa Cruz Biotechnology) was also performed but not quantified because <2 dilations/cyst per animal stained positive for the maker. Quantification was performed using ImageJ software, and cysts/tubular dilations were counted if their diameter exceeded 50 μm.

cAMP Analysis

Pieces from the flash-frozen left kidney were ground to fine powder and used for the cAMP assay as previously described following the manufacture's protocol (Enzo Life Sciences).[11]

Crude Membrane Preparation and Western Blotting

Huh7 and renal cortical tubular epithelial cells were cultured in DMEM media containing 10% FBS, penicillin/streptomycin, and glucose. Cells grown to confluence were washed three times with cold PBS, scraped and eluted in low-ionic-strength buffer (10 mM Tris HCL [pH, 7.4], 2.5 μl $MgCl_2$, 1 mM EDTA) containing protease inhibitor (Roche), and incubated for 30 minutes. Cells were then homogenized using a 26.5-gauge needle and nuclei were spun out at 2500 *g* for 5 minutes (4°C). The supernatant was collected and membrane fragments were pelleted at 20,000 *g* for 30 minutes (4°C). Pelleted membranes were eluted in low-ionic-strength buffer, and protein content was quantified using a bicinchoninic acid assay

(Thermo Fisher Scientific). For SDS PAGE, 25 μg (input ratio of 1) of membrane preparation was loaded onto a 3%–8% Tris-acetate gel (150 V for 2.5 hours). The gel was transferred to a polyvinylidene fluoride membrane and probed for PC1 (7e12, 1:1000) or PC2 (Yce2, 1:2000; Santa Cruz).

Statistical Analyses

All analyses were performed using JMP Pro 9. Comparisons between three or more groups were performed by 2-way ANOVA and least-squares means Tukey honest significant difference *post hoc* test (analyses of Figures 2 and 3, Supplemental Figure 1). Comparisons between two groups were performed by 2-way ANOVA and least-square means *t post hoc* test (analyses of Figure 1). Linear regression was used to test for potential synergism of tolvaptan and pasireotide, but the analysis was not significant (P=0.98). A P value below the α level of 0.05 was considered to represent a statistically significant difference. All data are represented as mean±SD.

ACKNOWLEDGMENTS

We would like to thank Drs. Scott L. Nyberg and Raymond Hickey (Department of Molecular Medicine, Mayo Clinic, Rochester, MN) for providing the Huh7 cell line and Otsuka Pharmaceuticals and Novartis for providing the tolvaptan and pasireotide used in this study.

This work was supported by National Institutes of Health grants DK44863 (V.E.T.), DK058816 (P.C.H.), and DK090728 (Mayo Translational PKD Center); the Zell Foundation; and the American Society of Nephrology Ben J. Lipps Research Fellowship (K.H.).

DISCLOSURES

None.

REFERENCES

1. Harris PC, Torres VE: Polycystic kidney disease, autosomal dominant. In: GeneReviews, edited by Pagon RA, Adam MP, Ardinger HH, Bird TD, Dolan CR, Fong CT, Smith RJH, Stephens K, Seattle, University of Washington, 1993 [Updated 2011]
2. Torres VE, Harris PC, Pirson Y: Autosomal dominant polycystic kidney disease. *Lancet* 369: 1287–1301, 2007
3. Nauli SM, Alenghat FJ, Luo Y, Williams E, Vassilev P, Li X, Elia AE, Lu W, Brown EM, Quinn SJ, Ingber DE, Zhou J: Polycystins 1 and 2 mediate mechanosensation in the primary cilium of kidney cells. *Nat Genet* 33: 129–137, 2003
4. Kusano E, Murayama N, Werness JL, Christensen S, Homma S, Yusufi AN, Dousa TP: Effects of calcium on the vasopressin-sensitive cAMP metabolism in medullary tubules. *Am J Physiol* 249: F956–F966, 1985
5. Kusano E, Yoshida I, Takeda S, Homma S, Yusufi AN, Dousa TP, Asano Y: Nephron distribution of total low Km cyclic AMP phosphodiesterase in mouse, rat and rabbit kidney. *Tohoku J Exp Med* 193: 207–220, 2001
6. Chabardès D, Imbert-Teboul M, Elalouf JM: Functional properties of Ca2+-inhibitable type 5 and type 6 adenylyl cyclases and role of Ca2+ increase in the inhibition of intracellular cAMP content. *Cell Signal* 11: 651–663, 1999
7. Yamaguchi T, Nagao S, Kasahara M, Takahashi H, Grantham JJ: Renal accumulation and excretion of cyclic adenosine monophosphate in a murine model of slowly progressive polycystic kidney disease. *Am J Kidney Dis* 30: 703–709, 1997
8. Gattone VH 2nd, Wang X, Harris PC, Torres VE: Inhibition of renal cystic disease development and progression by a vasopressin V2 receptor antagonist. *Nat Med* 9: 1323–1326, 2003
9. Smith LA, Bukanov NO, Husson H, Russo RJ, Barry TC, Taylor AL, Beier DR, Ibraghimov-Beskrovnaya O: Development of polycystic kidney disease in juvenile cystic kidney mice: Insights into pathogenesis, ciliary abnormalities, and common features with human disease. *J Am Soc Nephrol* 17: 2821–2831, 2006
10. Starremans PG, Li X, Finnerty PE, Guo L, Takakura A, Neilson EG, Zhou J: A mouse model for polycystic kidney disease through a somatic in-frame deletion in the 5′ end of Pkd1. *Kidney Int* 73: 1394–1405, 2008
11. Hopp K, Ward CJ, Hommerding CJ, Nasr SH, Tuan HF, Gainullin VG, Rossetti S, Torres VE, Harris PC: Functional polycystin-1 dosage governs autosomal dominant polycystic kidney disease severity. *J Clin Invest* 122: 4257–4273, 2012
12. Yamaguchi T, Pelling JC, Ramaswamy NT, Eppler JW, Wallace DP, Nagao S, Rome LA, Sullivan LP, Grantham JJ: cAMP stimulates the in vitro proliferation of renal cyst epithelial cells by activating the extracellular signal-regulated kinase pathway. *Kidney Int* 57: 1460–1471, 2000
13. Hanaoka K, Guggino WB: cAMP regulates cell proliferation and cyst formation in autosomal polycystic kidney disease cells. *J Am Soc Nephrol* 11: 1179–1187, 2000
14. Torres VE, Harris PC: Strategies targeting cAMP signaling in the treatment of polycystic kidney disease. *J Am Soc Nephrol* 25: 18–32, 2014
15. Chabardès D, Firsov D, Aarab L, Clabecq A, Bellanger AC, Siaume-Perez S, Elalouf JM: Localization of mRNAs encoding Ca2+-inhibitable adenylyl cyclases along the renal tubule. Functional consequences for regulation of the cAMP content. *J Biol Chem* 271: 19264–19271, 1996
16. Strait KA, Stricklett PK, Chapman M, Kohan DE: Characterization of vasopressin-responsive collecting duct adenylyl cyclases in the mouse. *Am J Physiol Renal Physiol* 298: F859–F867, 2010
17. Rieg T, Tang T, Murray F, Schroth J, Insel PA, Fenton RA, Hammond HK, Vallon V: Adenylate cyclase 6 determines cAMP formation and aquaporin-2 phosphorylation and trafficking in inner medulla. *J Am Soc Nephrol* 21: 2059–2068, 2010
18. Gattone VH 2nd, Maser RL, Tian C, Rosenberg JM, Branden MG: Developmental expression of urine concentration-associated genes and their altered expression in murine infantile-type polycystic kidney disease. *Dev Genet* 24: 309–318, 1999
19. Torres VE, Wang X, Qian Q, Somlo S, Harris PC, Gattone VH 2nd: Effective treatment of an orthologous model of autosomal dominant polycystic kidney disease. *Nat Med* 10: 363–364, 2004
20. Wang X, Gattone V 2nd, Harris PC, Torres VE: Effectiveness of vasopressin V2 receptor antagonists OPC-31260 and OPC-41061 on polycystic kidney disease development in the PCK rat. *J Am Soc Nephrol* 16: 846–851, 2005
21. Meijer E, Gansevoort RT, de Jong PE, van der Wal AM, Leonhard WN, de Krey SR, van den Born J, Mulder GM, van Goor H, Struck J, de Heer E, Peters DJ: Therapeutic potential of vasopressin V2 receptor antagonist in a mouse model for autosomal dominant polycystic kidney disease: optimal timing and dosing of the drug. *Nephrol Dial Transplant* 26: 2445–2453, 2011
22. Higashihara E, Torres VE, Chapman AB, Grantham JJ, Bae K, Watnick TJ, Horie S, Nutahara K, Ouyang J, Krasa HB, Czerwiec FS; TEMPOFormula and 156-05-002 Study Investigators: Tolvaptan in autosomal dominant polycystic kidney disease: Three years' experience. *Clin J Am Soc Nephrol* 6: 2499–2507, 2011
23. Torres VE, Chapman AB, Devuyst O, Gansevoort RT, Grantham JJ, Higashihara E, Perrone RD, Krasa HB, Ouyang J, Czerwiec FS; TEMPO 3:4 Trial Investigators: Tolvaptan in patients with autosomal dominant polycystic kidney disease. *N Engl J Med* 367: 2407–2418, 2012
24. Friedlander G, Amiel C: Somatostatin and alpha 2-adrenergic agonists selectively inhibit vasopressin-induced cyclic AMP accumulation in MDCK cells. *FEBS Lett* 198: 38–42, 1986

25. Ishikawa S, Saito T, Kuzuya T: Reversal of somatostatin inhibition of AVP-induced cAMP by pertussis toxin. *Kidney Int* 33: 536–542, 1988
26. Masyuk TV, Masyuk AI, Torres VE, Harris PC, Larusso NF: Octreotide inhibits hepatic cystogenesis in a rodent model of polycystic liver disease by reducing cholangiocyte adenosine 3′,5′-cyclic monophosphate. *Gastroenterology* 132: 1104–1116, 2007
27. Masyuk TV, Radtke BN, Stroope AJ, Banales JM, Gradilone SA, Huang B, Masyuk AI, Hogan MC, Torres VE, Larusso NF: Pasireotide is more effective than octreotide in reducing hepatorenal cystogenesis in rodents with polycystic kidney and liver diseases. *Hepatology* 58: 409–421, 2013
28. Ruggenenti P, Remuzzi A, Ondei P, Fasolini G, Antiga L, Ene-Iordache B, Remuzzi G, Epstein FH: Safety and efficacy of long-acting somatostatin treatment in autosomal-dominant polycystic kidney disease. *Kidney Int* 68: 206–216, 2005
29. van Keimpema L, Nevens F, Vanslembrouck R, van Oijen MG, Hoffmann AL, Dekker HM, de Man RA, Drenth JP: Lanreotide reduces the volume of polycystic liver: A randomized, double-blind, placebo-controlled trial. *Gastroenterology* 137: 1661–1668, 2009
30. Hogan MC, Masyuk TV, Page LJ, Kubly VJ, Bergstralh EJ, Li X, Kim B, King BF, Glockner J, Holmes DR 3rd, Rossetti S, Harris PC, LaRusso NF, Torres VE: Randomized clinical trial of long-acting somatostatin for autosomal dominant polycystic kidney and liver disease. *J Am Soc Nephrol* 21: 1052–1061, 2010
31. Caroli A, Perico N, Perna A, Antiga L, Brambilla P, Pisani A, Visciano B, Imbriaco M, Messa P, Cerutti R, Dugo M, Cancian L, Buongiorno E, De Pascalis A, Gaspari F, Carrara F, Rubis N, Prandini S, Remuzzi A, Remuzzi G, Ruggenenti P; ALADIN study group: Effect of longacting somatostatin analogue on kidney and cyst growth in autosomal dominant polycystic kidney disease (ALADIN): A randomised, placebo-controlled, multicentre trial. *Lancet* 382: 1485–1495, 2013
32. Walker BJ, Evans PA, Forsling ML, Nelstrop GA: Somatostatin and water excretion in man: an intrarenal action. *Clin Endocrinol (Oxf)* 23: 169–174, 1985
33. Vora JP, Owens DR, Ryder R, Atiea J, Luzio S, Hayes TM: Effect of somatostatin on renal function. *Br Med J (Clin Res Ed)* 292: 1701–1702, 1986
34. Reynaert H, Rombouts K, Vandermonde A, Urbain D, Kumar U, Bioulac-Sage P, Pinzani M, Rosenbaum J, Geerts A: Expression of somatostatin receptors in normal and cirrhotic human liver and in hepatocellular carcinoma. *Gut* 53: 1180–1189, 2004
35. Liu HL, Huo L, Wang L: Octreotide inhibits proliferation and induces apoptosis of hepatocellular carcinoma cells. *Acta Pharmacol Sin* 25: 1380–1386, 2004
36. Chapman AB, Bost JE, Torres VE, Guay-Woodford L, Bae KT, Landsittel D, Li J, King BF, Martin D, Wetzel LH, Lockhart ME, Harris PC, Moxey-Mims M, Flessner M, Bennett WM, Grantham JJ: Kidney volume and functional outcomes in autosomal dominant polycystic kidney disease. *Clin J Am Soc Nephrol* 7: 479–486, 2012
37. Wang X, Ye H, Ward CJ, Chu JY, Masyuk TV, Larusso NF, Harris PC, Chow BK, Torres VE: Insignificant effect of secretin in rodent models of polycystic kidney and liver disease. *Am J Physiol Renal Physiol* 303: F1089–F1098, 2012

This article contains supplemental material online at http://jasn.asnjournals.org/lookup/suppl/doi:10.1681/ASN.2013121312/-/DCSupplemental.